

# Hysteresis and ghost stationary currents in biased resonant tunneling heterostructures

Carlo Presilla<sup>a</sup> and Johannes Sjöstrand<sup>b</sup>

<sup>a</sup> *Dipartimento di Fisica, Università di Roma "La Sapienza," Piazzale A. Moro 2, 00185 Roma, Italy*

<sup>b</sup> *Centre de Mathématique, Ecole Polytechnique, F-91128 Palaiseau Cedex, France and U.A. 169, C.N.R.S. (cond-mat/9602047 submitted to Phys. Rev. Lett.)*

An adiabatic approximation in terms of instantaneous resonances is proposed to study the time dependent transport of interacting electrons in biased resonant tunneling heterostructures. In the case of a single resonance, we find current-voltage characteristics showing hysteresis or not in agreement with experimental results and predict the existence of ghost stationary currents linearly decaying in time.

03.65.-w, 73.40.Gk, 05.45.+b

From the early developments of resonant tunneling heterostructures, the electron-electron interaction has been supposed to have striking effects on the time dependent ballistic transport [1]. Currents oscillating at the picosecond scale [2] and quantum chaotic behavior without classical counterpart [3] have been predicted by accounting for the interaction at Hartree level. The difficult, although possible [4], experimental observation of these ballistic phenomena, contrasts with the simplicity of the conventional transport techniques making use of biased heterostructures. In this configuration, measurements usually probe stationary phenomena. For example, hysteresis in the current-voltage characteristics has been observed [5] and recognized as a consequence of the mutual interaction of the electrons trapped in the resonance [5,6,7,8]. Can signs of the electron-electron interaction be found also as time dependent phenomena occurring in biased heterostructures?

A first exploration in this direction was based on a fully numerical approach [9]. Here, we exploit a mathematical method, recently proposed in the framework of ballistic transport [10], which allows us to discuss both stationary and dynamical properties of biased heterostructures. At the stationary level, we obtain current-voltage characteristics in agreement with those measured in [11]. At the dynamical level, we predict the existence of ghost stationary currents, i.e., electrons trapped in the resonance whose decay is linear in time, which can survive up to the microsecond scale.

Let us consider a heterostructure whose conduction band profile consists of two barriers of height  $V_0$  located in  $[a, b]$  and  $[c, d]$  with  $a < b < c < d$  along the growth direction  $x$ . We are interested in evaluating the transport properties of this device when a bias  $\Delta V$  is applied between the emitter ( $x < a$ ) and collector ( $x > d$ ) regions uniformly doped. Doping allows for a continuous energy distribution of carriers in the emitter with Fermi

energy  $E_F = (3\pi^2 n_D)^{2/3}$ , where  $n_D$  is the net donor concentration. We will use everywhere effective atomic units  $\hbar = 2m^* = 1$  and  $e^2/\epsilon = 2$ , where  $m^*$  is the electron effective mass and  $\epsilon$  the dielectric constant. Assuming a decoupling between the degrees of freedom in the growth direction and in the plane parallel to the junctions, the time dependent Schrödinger equation for the single-electron wavefunction at energy  $E$  along the  $x$  direction is

$$[-i\partial_t - \partial_x^2 + V_{cb}(x) + U(\phi, x)] \phi(x, t, E) = 0 \quad (1)$$

where  $V_{cb}(x)$  is the step-like conduction band profile and  $U(\phi, x)$  takes into account the applied bias and, at Hartree level, the electron-electron interaction. Assuming ideal metallic behavior in the emitter and collector regions, i.e., neglecting the formation of accumulation and depletion layers,  $U(\phi, x)$  can be obtained as solution of the Poisson equation

$$\partial_x^2 U(\phi, x) = -8\pi \int dE g(E) |\phi(x, t, E)|^2 \quad (2)$$

with boundary conditions  $U(\phi, a) = 0$  and  $U(\phi, d) = -\Delta V$ . The factor

$$g(E) = \frac{\theta(E)}{2\pi} \left[ k_B T \ln \left( 1 + e^{\frac{E - E_F}{k_B T}} \right) + E_F - E \right] \quad (3)$$

takes into account the parallel degrees of freedom in the total electron density. In (3) the chemical potential at temperature  $T$  is approximated with the Fermi energy and the Heaviside function  $\theta(E)$  ensures that only energies above the bottom of the emitter conduction band,  $E = 0$ , are taken into account, as it is the case for  $E_F \ll \Delta V$ .

In general, the solution of (2) can not be handled analytically. We will suppose that, due to the accumulation of electrons in the well with sheet density

$$s(\phi) = \int dE g(E) \int_{(a+b)/2}^{(c+d)/2} dx |\phi(x, t, E)|^2, \quad (4)$$

ideal metallic behavior in the well  $[b, c]$  and ideal insulating behavior in the barriers  $[a, b]$  and  $[c, d]$  hold. Then the total potential  $V_{cb} + U$  in (1) is better rewritten as  $V + W$  where

$$V(x) = \begin{cases} 0 & x < a \\ V_0 - \Delta V(x - a)/\ell & a < x < b \\ -\Delta V(b - a)/\ell & b < x < c \\ V_0 - \Delta V(b - a + x - c)/\ell & c < x < d \\ -\Delta V & x > d \end{cases} \quad (5)$$

gives the band profile modified by the external bias and

$$W(s, x) = 8\pi s(\phi) \begin{cases} 0 & x < a \\ (x-a)(d-c)/\ell & a < x < b \\ (b-a)(d-c)/\ell & b < x < c \\ (b-a)(d-x)/\ell & c < x < d \\ 0 & x > d \end{cases} \quad (6)$$

depends on the wavefunction  $\phi$  through the sheet density of electrons in the well  $s(\phi)$ . Here  $\ell = b - a + d - c$ .

We will try to solve (1) with potential (5-6) in two steps. Let  $V_{\text{fill}}(x) = V(x) + V_0 1_{[b,c]}(x)$  be the potential obtained by filling the well  $[b, c]$ . Here  $1_{[b,c]}(x)$  is the characteristic function of the interval  $[b, c]$ . First we solve

$$[-i\partial_t - \partial_x^2 + V_{\text{fill}}(x) + W(s, x)] \tilde{\mu}(x, t, E) = 0 \quad (7)$$

and then we look for  $\phi$  in the form  $\phi = \tilde{\mu} + \tilde{\nu}$  where  $\tilde{\nu}$  should solve

$$[-i\partial_t - \partial_x^2 + V(x) + W(s, x)] \tilde{\nu}(x, t, E) = -V_0 1_{[b,c]}(x) \tilde{\mu}(x, t, E). \quad (8)$$

The wave function  $\tilde{\mu}$  describes an electron at energy  $E$  which is delocalized in the emitter and collector regions and has an exponentially small probability to be found in the forbidden region  $[a, d]$ . The wave function  $\tilde{\nu}$  describes the localization, driven by  $\tilde{\mu}$ , of the same electron in the well  $[b, c]$ . The wave function  $\phi$  of the original problem (1) can be approximated with  $\tilde{\nu}$  or  $\tilde{\mu}$  inside or outside the two barriers, respectively, with an error which is exponentially small in the limit of wide barriers [10,12].

Equation (7) can be solved by evaluating the instantaneous eigenstates of the potential  $V_{\text{fill}} + W$ . We put  $\tilde{\mu}(x, t, E) = \exp(-iEt)\mu(x, t, E)$  and suppose that  $\Delta V$  and  $s$  are slowly varying functions of time so that also  $\mu(x, t, E)$  is slowly varying in time. In the emitter region  $x < a$  we take  $\mu(x, t, E) = \mu(x, E)$  as the sum of a left- and right-going plane wave at energy  $E$  and propagate this expression to the adjacent regions by requiring  $\mu$  to be of class  $C^1$ . For wide barriers we can use a WKB expansion for the potential  $V_{\text{fill}} + W$  and explicitly determine  $\mu$  in the region  $[b, c]$  which is of interest for solving (8) [12].

Equation (8) can be simplified by developing  $\tilde{\nu}$  into the instantaneous eigenstates of the potential  $V + W$  and keeping only the contributions from the discrete resonant states, i.e., neglecting the contributions from the continuous spectrum [10]. We will suppose there is only one resonant state and put  $\tilde{\nu}(x, t, E) = \exp(-iEt)z(t, E)e(s, x)$  where  $e(s, x)$  is the (ground) resonant state of the potential  $V + W$

$$[-\lambda(s) - \partial_x^2 + V(x) + W(s, x)] e(s, x) = 0 \quad (9)$$

with complex eigenvalue  $\lambda(s) = E_R(s) - i\Gamma(s)/2$ . The eigenfunction  $e(s, x)$  is of class  $L^2$  on the contour  $\gamma \equiv$

$(e^{i\theta} - \infty, 0] + a) \cup [a, d] \cup (d + e^{i\theta}[0, +\infty[)$  for  $\theta$  conveniently chosen [13] and satisfies

$$\int_{\gamma} dx e(s, x)^2 = 1, \quad \int_{\gamma} dx e(s, x) \partial_s e(s, x) = 0. \quad (10)$$

Multiplying (8) with  $e(s, x)$  and integrating over  $\gamma$ , we get

$$\partial_t z(t, E) = i[E - \lambda(s)] z(t, E) + \mathcal{B}(s, E) \quad (11)$$

with the driving term given by

$$\mathcal{B}(s, E) = iV_0 \int_b^c dx \mu(x, t, E) e(s, x) \quad (12)$$

and the sheet density (4) reduced, with small error, to

$$s = \int dE g(E) |z(t, E)|^2 \equiv \|z(t)\|^2. \quad (13)$$

Explicit expressions of  $\lambda(s)$  and  $e(s, x)$  can be found within the same WKB approximation used for evaluating  $\mu$  [12]. For later use we note that  $E_R(s) = E_R^0 + \eta s$ , where  $E_R^0 = E_0 - \Delta V(b-a)/\ell$ ,  $E_0$  is the (ground) eigenstate of the potential  $V_0 [1_{[-\infty, b]}(x) + 1_{[c, +\infty]}(x)]$  and  $\eta$  a positive constant [12].

The original problem (1) is reduced to solve the system (11) with the condition (13) which couples the amplitudes  $z(t, E)$  with different energy. Let us first consider the stationary fixed point solutions of (11)

$$z_{\text{fix}}(E) = \frac{\mathcal{B}(s, E)}{-\Gamma(s)/2 + i[E - E_R(s)]}. \quad (14)$$

Equation (13) gives a self-consistency condition for  $s = \|z_{\text{fix}}\|^2$ . Assuming that  $|\mathcal{B}(s, E)|^2$  is a smooth function of  $E$  and  $\Gamma(s) \ll E_F$ , a Dirac  $\delta$  approximation can be used to get

$$s = f(s) \equiv 2\pi \frac{g(E_R(s)) |\mathcal{B}(s, E_R(s))|^2}{\Gamma(E_R(s))}. \quad (15)$$

The function  $f(s)$  vanishes everywhere except for  $0 \leq E_R^0 + \eta s \lesssim E_F$  where it looks like a regular bump with a square root singularity at the left end point. Therefore, Eq. (15) has only one solution for  $E_R^0 \geq 0$  and may have three for  $E_R^0 < 0$ . For  $E_R^0 \gtrsim E_F$  the unique solution vanishes and for  $E_R^0 < 0$  the couple of nonvanishing solutions is to be searched in the interval  $-E_R^0/\eta \leq s \lesssim (-E_R^0 + E_F)/\eta$ . The existence of this couple of solutions depends on the amplitude of the function  $f$ . In the case of asymmetric barriers, if the emitter barrier  $[a, b]$  is narrower than the collector one  $[c, d]$  the resonance width  $\Gamma$ , determined by the narrower barrier, is of the same order as the driving term  $|\mathcal{B}|^2$ , determined by the emitter barrier, and  $f \sim g$ . Due to the shape of  $g$ , three solutions of (15) exist for a proper value of  $E_R^0$ , i.e.,  $\Delta V$ . On the other hand, if the emitter barrier

is wider than the collector one the driving term  $|\mathcal{B}|^2$  is exponentially suppressed and (15) always has only one solution.

The solutions of (15) can be characterized in terms of stability. By studying the eigenvalues of the linearization of the vector field defined by the r.h.s. of (11) one can demonstrate that a solution of (15) is stable (unstable) when  $\partial_s f(s) < 1$  ( $> 1$ ) [12]. The trivial solution  $s = 0$ , when it exists, is, therefore, a stable one. When three solutions exist, two of them, the largest and the smallest one, are stable while the intermediate one is unstable.

The stable solutions of (15) are the values of the sheet density of electrons in the well which can be expected as result of a stationary measurement. Analogous considerations hold for the collector electric current  $I = e A_s J(s)$ , proportional to the number of electrons in the well,  $A_s$ ,  $A$  being the lateral area of the device, and to the probability current density of the resonant state at  $x = d^+$ ,  $J(s) = 2\sqrt{E_R(s) + \Delta V}|e(s, d^+)|^2$ .

A good test for our  $I(\Delta V)$  is the comparison with the current-voltage characteristics measured in an asymmetric double-barrier heterostructure under forward and reverse bias [11]. The parameters of the GaAs-AlGaAs heterostructure of [11] are  $n_D = 2 \times 10^{-17} \text{ cm}^{-3}$ ,  $T = 1 \text{ K}$ ,  $A = 2 \times 10^{-5} \text{ cm}^2$ ,  $c - b = 56 \text{ \AA}$  and barriers with the same width,  $90 \text{ \AA}$ , but different Al concentration, i.e., different heights,  $0.34$  and  $0.48 \text{ eV}$ , according to [15]. We simulate this asymmetry by choosing equal-height different-width barriers having equivalent opacity, i.e.,  $V_0 = 0.34 \text{ eV}$ ,  $b - a = 90 \text{ \AA}$  and  $d - c = 107 \text{ \AA}$ . We also take  $m^* = 0.067 m$ , where  $m$  is the free electron mass, and  $\varepsilon = 11.44$  [15]. Figure 1 shows the  $I(\Delta V)$  curve obtained with the chosen parameters (right-most curve) or by exchanging  $b - a$  and  $d - c$  (left-most curve). In agreement with the above discussion no multiple solutions are seen in the left-most curve (reverse bias case) when the emitter barrier is wider than the collector one. On the other hand, in the forward bias case a bistable region is observed between points A and B. These facts, as well as the magnitude of the peak currents shown in Fig. 1 are in agreement with the experiment [11]. Of course, the bias scale of Fig. 1 can not be compared with that in the experiment due to the accumulation and the depletion layers [14] neglected in our model. Moreover, the valley current of our model is the trivial solution  $I = 0$ . A more realistic valley current is obtained by numerically evaluating the integral (13) with no approximations [12].

Now we turn to the time-dependent transport properties. According to (11) and (13), the dynamical equation for the sheet density of electrons in the well is

$$\begin{aligned} \partial_t s(t) &\equiv \partial_t \|z(t)\|^2 = 2\text{Re}\langle z | \partial_t z \rangle \\ &= -\Gamma(s(t)) s(t) + 2\text{Re}\langle z | \mathcal{B} \rangle \end{aligned} \quad (16)$$

where  $\langle u | v \rangle \equiv \int dE g(E) \overline{u(E)} v(E)$ . The last term in (16) can be expressed in terms of  $s(t)$  by using the formal

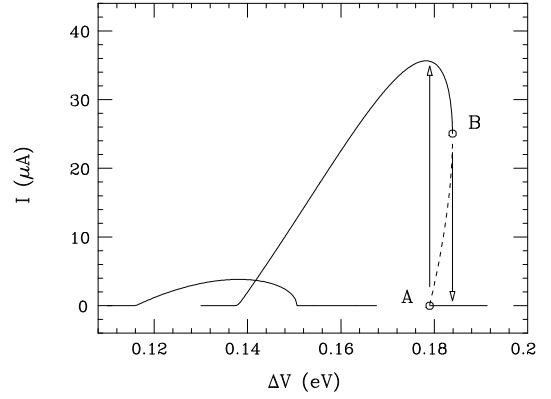


FIG. 1. Stationary current *versus* applied bias for the asymmetric double barrier heterostructure described in the text and reproducing the experiment [11] under forward (right-most curve) and reverse (left-most curve) bias. In the reverse bias case we permuted the barriers instead of making  $\Delta V$  (and  $I$ ) negative. In the forward bias case the dashed line is an unstable fixed point solution and the arrows indicate the transition expected at points A and B by decreasing or increasing the bias, respectively.

solution of (11)

$$\begin{aligned} z(t, E) &= e^{\int_0^t dt' [-\frac{1}{2}\Gamma(s(t')) + i(E - E_R(s(t')))]} z(0, E) + \\ &\int_0^t dt' e^{\int_{t'}^t dt'' [-\frac{1}{2}\Gamma(s(t'')) + i(E - E_R(s(t'')))]} \mathcal{B}(s(t'), E). \end{aligned} \quad (17)$$

The first term in (17) vanishes exponentially and can be neglected after a time  $t \gg 2/\Gamma$ . In the second term, an analogous exponential factor selects the contributions for  $t - t' \lesssim 2/\Gamma$  as the dominant ones so that the lower integration bound can be safely changed into  $-\infty$  for  $t \gg 2/\Gamma$ . In this case we have

$$\begin{aligned} 2\text{Re}\langle z | \mathcal{B} \rangle &= \\ 2\text{Re} \int_{-\infty}^t dt' e^{\int_{t'}^t dt'' [-\frac{1}{2}\Gamma(s(t'')) + iE_R(s(t''))]} g|\widehat{\mathcal{B}}|^2 (t - t') & \\ \simeq 2\text{Re} \int_{-\infty}^t dt' e^{iE_R(s(t))(t-t')} g|\widehat{\mathcal{B}}|^2 (t - t') & \\ = 2\pi g(E_R(s(t))) \mathcal{B}(s(t), E_R(s(t))). & \end{aligned} \quad (18)$$

Here  $g|\widehat{\mathcal{B}}|^2$  is the Fourier transform obtained by performing the energy integral in the scalar product and the approximation in the third line is valid for  $\Gamma$  and  $\partial_t s(t)$  small [12]. With this result Eq. (16) becomes

$$\partial_t s(t) = -\Gamma(s(t)) \left( s(t) - f(s(t)) \right) \quad (19)$$

which is very simple to handle numerically. The fixed point solutions  $s = \|z_{\text{fix}}\|^2$  of (19) coincide with those defined by (15) and also their attractive nature agrees with the stability condition discussed above.

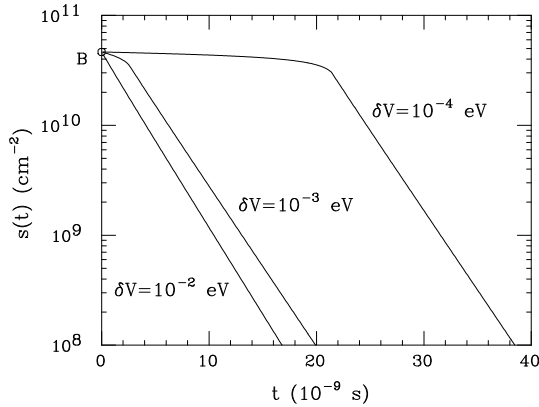


FIG. 2. Sheet density of electrons in the well  $s(t)$  after an instantaneous bias increase  $\delta V$  from the point  $B$  of Fig. 1.

Figure 2 shows the evolution of the sheet density  $s(t)$  for a perturbation of the stable fixed point solution at point  $B$  of Fig. 1. At time  $t = 0$  the bias  $\Delta V$  is increased by  $\delta V$  and  $s(t)$  forced to move toward the new unique stable fixed point solution. However, we see that for  $\delta V \rightarrow 0$  a ghost fixed point solution survives for some time, the two opposite terms in (19) nearly compensate and  $s(t)$  decreases linearly. When  $E_R(s(t))$  becomes negative,  $f = 0$  and  $s(t)$  decays exponentially. The condition  $E_R(s(t)) = 0$  defines, therefore, the survival time  $t_g$  of the ghost fixed point solution.

An approximate description of the ghost solution can be obtained by rewriting (19) as  $\partial_t s(t) = h(s, \delta V)$  and observing that for  $s(t) - s(0)$  and  $\delta V$  small we must have  $h(s, \delta V) \simeq -q[s(t) - s(0)]^2 - p\delta V$  with  $q, p > 0$ . Integrating, we obtain  $s(t) = s(0) - \sqrt{\delta V p/q} \tan(\sqrt{qp\delta V} t)$  which has linear behavior for small  $t$ . Inverting this solution and assuming  $\sqrt{\delta V p/q} \ll s(0) - s(t_g)$  we estimate  $t_g \sim \delta V^{-1/2}$ . This behavior is verified in Fig. 3, where the ghost survival time is plotted as a function of  $\delta V$ .

The ghost fixed point solutions shown in Figs. 2 and 3 have been obtained through the approximate Eq. (19). This approximation, however, is fully appropriate to that purpose since we have  $t_g \gg \Gamma^{-1} \sim 10^{-9}$  s. This is confirmed by a comparison with the exact results obtained by numerically solving (11) on a proper time-energy lattice [12]. The exact numerical approach allows us also to study the ghost current obtained by decreasing the bias from point  $A$  of Fig. 1. Due to the square root singularity of the function  $f(s)$  at  $s = -E_R^0/\eta$ , the survival time of this ghost is much shorter than that shown in Fig. 2 and the approximation (19) is not appropriate.

According to Fig. 3, dynamical measurements of the ghost currents related to the electron-electron interaction are within the reach of present technology. More complex nonequilibrium features can be expected in heterostructures with many resonances [12] or in superlattices [16,17].

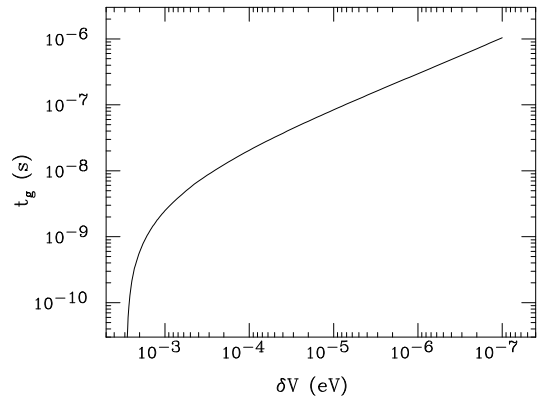


FIG. 3. Survival time  $t_g$  of the ghost fixed-point solution of Fig. 2 as a function of the bias increase  $\delta V$ .

It is a pleasure to thank G. Jona-Lasinio for stimulating discussions, as well as G. Perelman, who independently observed how to get (19) from (16). Partial support of INFN, Iniziativa Specifica RM6, is acknowledged.

- 
- [1] B. Ricco and M. Ya. Azbel, Phys. Rev. B **29**, 1970 (1984).
  - [2] C. Presilla, G. Jona-Lasinio, and F. Capasso, Phys. Rev. B **43**, 5200 (1991).
  - [3] G. Jona-Lasinio, C. Presilla, and F. Capasso, Phys. Rev. Lett. **68**, 2269 (1992).
  - [4] T. Sajoto, J. J. O'Shea, S. Bhargava, D. Leonard, M. A. Chin, and V. Narayanamurti, Phys. Rev. Lett. **74**, 3427 (1995).
  - [5] V. J. Goldman, D. C. Tsui, and J. E. Cunningham, Phys. Rev. Lett. **58**, 1256 (1987).
  - [6] F. W. Sheard and G. A. Toombs, Appl. Phys. Lett. **52**, 1228 (1988); Semicond. Sci. Technol. **7**, B460 (1992).
  - [7] A. N. Korotkov, D. V. Averin, and K. K. Likharev, Physica B **165** & **166**, 927 (1990).
  - [8] Y. Abe, Semicond. Sci. Technol. **7**, B498 (1992).
  - [9] K. L. Jensen and F. A. Buot, Phys. Rev. Lett. **66**, 1078 (1991).
  - [10] G. Jona-Lasinio, C. Presilla, and J. Sjöstrand, Ann. Phys. **240**, 1 (1995).
  - [11] A. Zaslavsky, V. J. Goldman, D. C. Tsui, and J. E. Cunningham, Appl. Phys. Lett. **53**, 1408 (1988).
  - [12] J. Sjöstrand and C. Presilla, submitted to J. Math. Phys..
  - [13] J. Aguilar and J. M. Combes, Comm. Math. Phys. **22**, 269 (1971).
  - [14] V. J. Goldman, D. C. Tsui, and J. E. Cunningham, Phys. Rev. **35**, 9387 (1987).
  - [15] R. Atanasov and F. Bassani, Solid State Comm. **84**, 71 (1992).
  - [16] J. Kastrup, H. T. Grahn, K. Ploog, F. Prengel, A. Wacker, and E. Schöll, Appl. Phys. Lett. **65**, 1808 (1993).
  - [17] N. G. Sun and G. P. Tsironis, Phys. Rev. B **51**, 11221 (1995).